

Open-path trace gas detection of ammonia based on cavity-enhanced absorption spectroscopy

R. Peeters¹, G. Berden¹, A. Apituley³, G. Meijer^{1,2}

¹Department of Molecular and Laser Physics, University of Nijmegen, Toernooiveld, NL-6525 ED Nijmegen, The Netherlands (Fax: +31-243/653-311, E-mail: rudyp@sci.kun.nl)

²FOM-Institute for Plasma Physics Rijnhuizen, P.O. Box 1207, NL-3430 BE Nieuwegein, The Netherlands

³National Institute of Public Health and Environment (RIVM), P.O. Box 1, NL-3720 BA Bilthoven, The Netherlands

Received: 19 January 2000/Revised version: 6 March 2000/Published online: 7 June 2000 – © Springer-Verlag 2000

Abstract. A compact open-path optical ammonia detector is developed. A tunable external-cavity diode laser operating at 1.5 μm is used to probe absorptions of ammonia via the cavity-enhanced absorption (CEA) technique. The detector is tested in a climate chamber. The sensitivity and linearity of this system are studied for ammonia and water at atmospheric pressure. A cluster of closely spaced rovibrational overtone and combination band transitions, observed as one broad absorption feature, is used for the detection of ammonia. On these molecular transitions a detection limit of 100 ppb (1 s) is determined. The ammonia measurements are calibrated independently with a chemiluminescence monitor. Compared to other optical open-path detection methods in the 1–2 μm region, the present result shows an improved sensitivity for contactless ammonia detection by over one order of magnitude. Using the same set-up, a detection limit of 100 ppm (1 s) is determined for the detection of water at atmospheric pressure.

PACS: 07.57.Ty; 07.07.Df; 07.88.+y; 33.20.Ea

Industrial emissions and intensive livestock breeding are dominant contributors to the total amount of ammonia in the atmosphere. The ambient concentration and the time-integrated deposition of ammonia are important parameters in acidification and eutrophication processes. These processes can result in environmental damaging effects and in public health hazards. It is therefore necessary to map out and control the ammonia emissions and depositions. Hence, fast (> 1 Hz), sensitive (sub-ppb) and non-intrusive ammonia detectors capable of measuring ammonia in ambient air are indispensable.

Most of the commercially available ammonia monitors use chemical, thermochemical, or optochemical detection schemes and require the collection of atmospheric samples. Their sensitivity ranges from 1 ppt (chemical, thermochemical) [1] to 1 ppm (optochemical) but their response time,

however, is usually long and, above all, their intrusive properties are unwanted for several applications. The sampling of air prohibits contactless measurements and, due to the adhesive properties of ammonia, long-term memory effects can introduce measurement errors.

These drawbacks can be circumvented by using the optical properties of the ammonia molecule. A measurement of the molecular absorption spectrum provides information about the ammonia concentration in the probed volume. Over the years various optical detection schemes have been developed and used with the aim to construct a highly sensitive ammonia monitor. High detection sensitivities have been achieved using opto-acoustical techniques with detection limits in the low ppb range [2–6]. Nevertheless, these methods still require the sampling of gas and thus are not suitable for open-path monitoring of ammonia.

The use of diode lasers for trace-gas detection offers various advantages, among which are their narrow laser bandwidth with the associated high frequency and species selectivity. Moreover, they are very compact, easy to use, and affordable. These qualities make them well suited for the implementation in laser-based trace-gas detection systems. Diode lasers are commercially available throughout the 0.7–2.0 μm region, where many trace-gas species of interest have rovibrational transitions. The rovibrational line strengths in these combination and overtone bands are weak compared to the line strengths in the fundamental bands, and highly sensitive detection schemes are therefore needed.

For ammonia many vibrational bands have been reported in the 1–2 μm region [7–10]. On the basis of motives such as the line strength of the absorptions and the avoidance of interference with other atmospheric gases, different combination and overtone bands of ammonia have been chosen for the construction of an open-path ammonia sensor. This resulted in best detection limits of 2 ppm under atmospheric conditions in the 1.5- μm band [11–14] and of 55 ppm at a total pressure of 76 Torr in the 1.65- μm region [15]. Recently, new diode lasers operating in the 2.0- μm region have been used for the detection of ammonia and a detection limit

of 1 ppm has been demonstrated [16, 17]. These sensitivities have been achieved by using a diode laser system in combination with advanced measurement schemes such as (two-tone) frequency modulation.

Recently, we have reported on the cavity-enhanced absorption (CEA) technique, a versatile and sensitive tool for spectroscopic studies [10, 18]. With this technique, rotational transitions of the $b^1\Sigma_g^+(v' = 2) \leftarrow X^3\Sigma_g^-(v'' = 0)$ band of molecular oxygen have been measured around 628 nm [18]. Additionally, a sensitivity of 10^{-6} mbar for the detection of ammonia under reduced background pressure was demonstrated in the 1.5- μm band. The CEA technique has been successfully combined with magnetic rotation spectroscopy to obtain cavity-enhanced magnetic rotation spectra of the $^P P_1(1)$ transition of the aforementioned, magnetic-dipole-allowed, band of molecular oxygen. Absorption features narrower than 270 MHz can be recorded, as was shown by measuring the $^P P_1(1)$ transition of the $b^1\Sigma_g^+(v' = 0) \leftarrow X^3\Sigma_g^-(v'' = 0)$ band of molecular oxygen in an optical cavity positioned around a slit-jet expansion [18]. With the same set-up, we have recorded absorption spectra of rotationally cold ammonia molecules in the 6400–6630 cm^{-1} region, enabling us to assign all of the lower rotational transitions of the $\nu_1 + \nu_3$ band and of the $|l| = 2$ component of the $\nu_1 + 2\nu_4$ band of ammonia [10].

In this paper, we report on the design and performance characteristics of our compact and open-path ammonia sensor based on CEA spectroscopy. An external-cavity diode laser (ECDL) is used to probe ammonia absorptions in the 1.5- μm region. The ammonia sensor is tested and calibrated in a climate chamber [19]. A test-gas generator is used to mix predetermined concentrations of ammonia with air in a well-controlled and reproducible way. The ammonia concentration is calibrated independently using a chemiluminescence monitor. It is shown that with a simple set-up involving CEA a sub-ppm detection limit for ammonia is readily achieved.

1 Theory

The CEA technique is already described elsewhere [18], and only the main principles of the technique will be given here. Light of a scanning laser is coupled into a high-finesse optical cavity when the frequency of the light is in resonance with the frequency of one of the cavity modes. In this experiment the laser is continuously scanned over the same spectral region (typically 1 cm^{-1}), and at the same time the length of the optical cavity is periodically changed with a piezo-element that scans the mode spectrum over one free spectral range (FSR). As a result, different laser frequencies can be coupled into the cavity each subsequent single scan ('interleaved sampling'). By summing over several single scans, each frequency will be sampled with an equal probability and spectral features narrower than the FSR of the cavity can be studied.

The intensity of the light coupled into the optical cavity is determined by the spectral overlap between the laser frequency and the frequency of the matching cavity mode, and depends on the finesse of the cavity, the spectral profile of the laser, the scanning rate of the laser frequency, and the scanning rate of the cavity length by the piezo on the end-mirror. The scanning rates must be set in such a way that the laser frequency stays in resonance with the cavity mode sufficiently

long, resulting in a maximum intensity that is proportional to the exponential decay time $\tau(\nu)$,

$$\tau(\nu) = \frac{d}{c(1 - R + \kappa(\nu)d)}, \quad (1)$$

where d is the cavity length, c is the speed of light, R the mirror reflectivity, and $\kappa(\nu)$ the absorption coefficient of an absorbing species inside the cavity. This restriction sets the upper limit for the scanning rate of the laser frequency. In addition there also is a restriction to the lower limit of the scanning rate of the laser. Apart from the periodic change of the cavity length controlled by the piezo-element, there will also be an additional jittering of the cavity modes due to the mechanical instability of the cavity. In order to minimise the intensity fluctuations inside the cavity, all laser frequencies must be in resonance with a cavity mode equally long and the scanning rate of the laser must therefore be significantly higher than the rate at which the cavity modes are jittering. When both of these restrictions are fulfilled, the intensity coupled into the cavity is linearly dependent on $\tau(\nu)$. Furthermore, when the laser is tuned out of resonance with the cavity mode, the intensity inside the cavity shows an exponential decay in time, also proportional to $\tau(\nu)$. In a CEA experiment, the *time-integrated* intensity of the light exiting the cavity is measured. This signal is proportional to the exponential decay time $\tau(\nu)$, and thus contains information on the absorption coefficient $\kappa(\nu)$, which is the product of the concentration and the absorption cross-section of the absorbing species in the cavity. By plotting the inverse of the time-integrated detector signal versus the frequency of the laser, an absorption spectrum over the full scanning range of the laser is obtained.

2 Experiment

A scheme of the CEA experiment is depicted in Fig. 1. A continuous-wave ECDL (New Focus, model 6262), operating in the 1512–1590 nm region with a 5-mW maximum power and a laser bandwidth narrower than 5 MHz, is used as a light source. Temperature, current, and frequency of the laser are regulated with an external controller. The frequency region of interest can be attained by adjusting the end-mirror of the laser cavity with a pico-motor. During the measurement, the laser is scanned mode-hop free, and linearly in time, over 1 cm^{-1} frequency intervals. It is important that the full spectral range is covered rather fast, in this particular case at a rate of 32 Hz. This is done by applying a voltage ramp to the piezo-electric transducer that is connected to the end-mirror of the laser cavity.

The light of the laser is coupled into a high-finesse optical cavity formed by two plano-concave mirrors with a specified reflectivity R of 0.9997, a diameter of 25 mm, and a radius of curvature r equal to -1 m. Optical feedback from the cavity back to the laser is minimized by a Faraday isolator placed in the beam directly behind the laser aperture. The mirrors are mounted in two mirror-holders that can be aligned independently. The distance d between the two mirrors is 65 cm. The exact cavity length is continuously varied by a piezo-element fixed to the end-mirror in such a way that the cavity mirror will travel one wavelength in one full piezo-scan (scan rate typically 0.5 Hz). This is equivalent to an 'active destabilization' of the detection cavity, and enhances the efficiency with

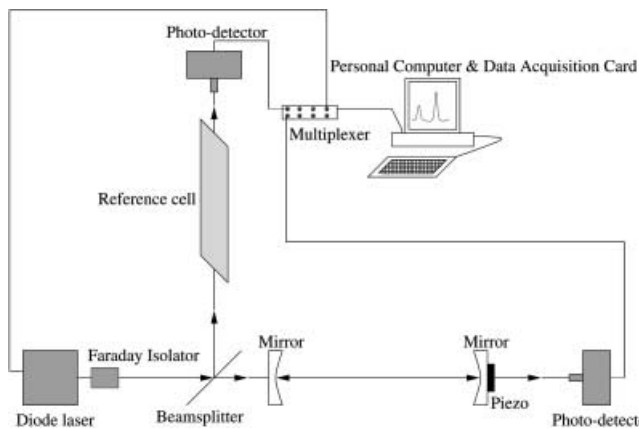


Fig. 1. Experimental set-up for cavity-enhanced absorption spectroscopy. Light from the scanning laser is split in two beams one of which is coupled into a high-finesse optical cavity and the other is led through an 18-cm-long reference cell containing 9-Torr ammonia used for frequency calibration. The light exiting the high-finesse cavity is detected with a photodiode and the time-integrated signal is used to extract information about the absorbing species that are present in this cavity

which the narrow-band laser light is coupled into this cavity. The light exiting the cavity at the end mirror is detected with a photodetector (New Focus, Nirvana 2017) which is connected to an analog input of a multiplexer (National Instruments, BNC 2090). The data is transferred to a personal computer via a data acquisition card (National Instruments, PCI-MIO-E 16) using LabView-based acquisition software. The intensity of the light exiting the cavity is recorded and displayed as a function of the scanning voltage of the laser which is proportional to the laser frequency.

The absolute laser frequency is calibrated by measuring a direct absorption spectrum of 9 Torr NH_3 in a cell simultaneously with the CEA spectrum. Most of the ammonia absorption frequencies in the $1.5\text{-}\mu\text{m}$ region have been accurately measured and reported by Lundsberg-Nielsen et al. [9]. Since the ammonia spectrum is very dense and complex, the different frequency regions show distinct patterns of absorption lines. Therefore, using the known line positions and line strengths, the absolute frequency of the diode laser can easily be determined.

In order to test the CEA-based ammonia detector in an open-path set-up, and to control the ammonia concentration in the probed volume, the CEA system is enclosed in a large Perspex box. The complete set-up is placed inside a climate chamber [19], where a test-gas generator supplies a continuous flow of air with a known composition mixed with a pre-determined concentration of ammonia gas. A scheme of the manifold including the CEA detector is shown in Fig. 2. In the gas generator, compressed air is cooled down to $2\text{ }^\circ\text{C}$ and liquid water is separated from the gas system. The air is purified in a heatless dryer consisting of two columns filled with silica gel and charcoal. The dried air flow can be mixed up with a known amount of water in the atomizer. The ammonia is added to the air and the gas composition is led via a Teflon-lined manifold into the perspex box enclosing the CEA detector at a flow rate of $0.501/\text{min}$. A relative humidity sensor is used to measure the water vapour concentration in the supplied gas mixture. Additionally, air from inside the box is sampled and transferred to an oven ($800\text{ }^\circ\text{C}$) in which the ammonia is converted to NO_x , that in turn is detected by

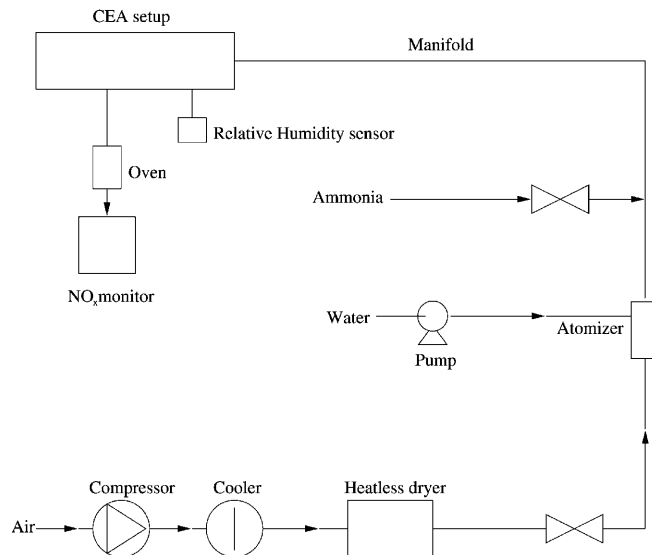


Fig. 2. Test-gas generator used to supply a continuous flow of air with a pre-determined concentration of ammonia gas. Air is first purified and mixed with concentrations of water and ammonia. This gas mixture is led via a Teflon-lined manifold to the CEA detector enclosed in a large Perspex box. The ammonia and water concentration in the box are independently measured with a chemiluminescence monitor and a relative humidity sensor, respectively

a chemiluminescence monitor. The ammonia and the water signal measured with the CEA ammonia sensor can thus be calibrated independently.

3 Results and discussion

Lundsberg-Nielsen et al. [9] have reported a total of 1810 rovibrational ammonia lines in the $1.5\text{-}\mu\text{m}$ region, originating from a multitude of combination and overtone bands [7, 8, 10] from which our ECDL can reach approximately 700 lines. For the present studies, we choose the closely spaced cluster of ammonia lines at 6568.299 , 6568.401 , and 6568.463 cm^{-1} with absorption coefficients of 7.556×10^{-4} , 7.602×10^{-4} , and $0.948 \times 10^{-4}\text{ cm}^{-1}\text{ Torr}^{-1}$, respectively [9]. Under ambient conditions these three lines blend into a broad absorption feature, one of the most intense ammonia features in the frequency region accessible to the laser. Furthermore, this is an isolated cluster of lines as the nearest ammonia absorption is more than 0.5 cm^{-1} away. Therefore, it is possible to scan the laser over 1 cm^{-1} without probing ammonia lines that will interfere with the lines under study, as is the case in other frequency regions where absorptions with comparable line strengths could in principle be used as well.

In Fig. 3a a direct absorption spectrum of 9-Torr ammonia in an 18-cm cell measured in the reference path is shown. The three closely spaced rotational lines are clearly visible and at the red side of the first strong line a very weak, hitherto unreported, absorption feature is seen. The linewidth is a result of both the Doppler-broadening ($\approx 0.02\text{ cm}^{-1}$) and pressure-broadening due to ammonia (self-broadening; $\approx 20\text{ MHz/Torr}$).

In the CEA measurements, a low ammonia concentration is measured in air at atmospheric pressure. The relative humidity of the gas mixture is zero. In Fig. 3b the CEA absorp-

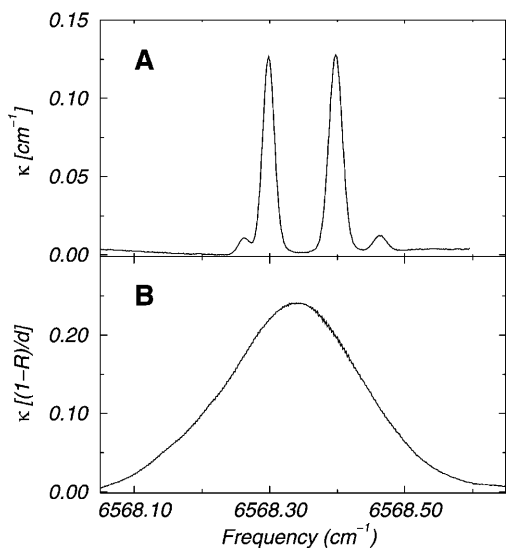


Fig. 3. **a** Direct absorption spectrum of 9-Torr ammonia measured in the 18-cm-long reference cell. A cluster of four closely spaced rovibrational transitions is seen. **b** CEA measurement of 1.2-ppm ammonia at atmospheric pressure. The relative humidity in the gas mixture is zero. The spectrum is obtained in 8 s. The four separate rovibrational transitions now form one broad absorption feature. The line width is predominantly governed by the pressure broadening by air

tion spectrum of 1.2 ppm ammonia is shown. The spectrum is the average of 256 scans and is acquired in 8 s. The frequency axis is linearized using the direct absorption spectrum as a reference. The absorption coefficient $\kappa(\nu)$ is expressed in units of $(1 - R)/d$. In order to make this vertical scale absolute, the reflectivity of the mirrors has to be known precisely. Alternatively, the vertical axis can be calibrated with a known molecular absorption (*vide infra*). In this experiment, the CEA signal is calibrated independently using the ammonia concentration detected with the chemiluminescence monitor.

As the ammonia concentration is very low, self-broadening does not contribute noticeably to the spectral linewidth. The dominant contributor to the observed linewidth is pressure broadening by air, which is approximately 6 MHz/Torr. The CEA spectrum can be obtained by convoluting the low-pressure spectrum with a Lorentz profile. However, it is readily seen that the center of the broad absorption feature is not at the center of the two strong narrow lines in the cell spectrum. This is a result of the pressure-shift of the rovibrational lines. A detailed study showed that there is a non-equal shift for the 6568.299 cm^{-1} and the 6568.401 cm^{-1} absorptions of $\approx 0.8 \text{ MHz/Torr}$ and $\approx 0.2 \text{ MHz/Torr}$, respectively. Therefore, their frequency separation will decrease under atmospheric conditions, which results in a narrower CEA feature.

Prior to the measurement of an ammonia spectrum it is important to wait for the ammonia concentration in the gas flow to stabilize. Due to the strong adhesive properties of ammonia, part of the gas will easily stick to the system surfaces. In addition, desorption from these surfaces will occur as well. The combination of these two effects will cause an additional variation of the ammonia concentration in the gas flow every time the concentration is changed. When the read-out value of the chemiluminescence monitor is constant (within 5 ppb) for

about ten min, the concentration in the gas flow is assumed to be stable and the actual measurement is started. After each session, the system is flushed with dry air in order to dispose of the residual ammonia in the system.

The linearity of the CEA detector is studied by varying the ammonia concentration in the air flow. The results are shown in Fig. 4. On the horizontal axis the ammonia concentration measured with the chemiluminescence monitor is plotted and on the vertical axis the integrated absorption S , which is the area under the detected absorption feature, is plotted. From Fig. 4 a linear dependence between the integrated CEA signal and the supplied concentration is evident. The detection limit defined as the concentration that results in a signal-to-noise ratio (SNR) equal to 1, is 100 ppb (1 s). This corresponds to a fractional absorption of $2 \times 10^{-8} \text{ cm}^{-1}$. The noise in the CEA spectrum is determined by the residual mode structure, which is a result of the interaction of the cavity modes and the variation of the bandwidth and the power of the laser in the wavelength scans [18].

Interferences of water and carbon dioxide can limit the detection of ammonia. Although the line strengths of these molecules are substantially weaker than for ammonia, these species are far more abundant in the atmosphere ($\approx 10\,000 \text{ ppm}$ and $\approx 360 \text{ ppm}$, respectively). For field measurements, it is therefore important to choose ammonia absorptions that are free from interferences. For the frequency range shown in Fig. 3b an interfering water absorption at 6568.407 cm^{-1} with a line strength of $9.6 \times 10^{-6} \text{ cm}^{-2} \text{ atm}^{-1}$ has been reported [20]. In order to verify the line position and line strength of this water absorption, we recorded the CEA spectrum of 1 mbar water in a cell. The measurements (not shown) are in agreement with the reported values. In the $1.5\text{-}\mu\text{m}$ region there are several interference free ammonia absorptions which can easily be selected. The sensitivity of the CEA technique scales linearly with the absorption cross-section and can thus be determined for the selected transition.

In order to test the linearity of the CEA detector over a larger range than depicted in Fig. 4, higher concentra-

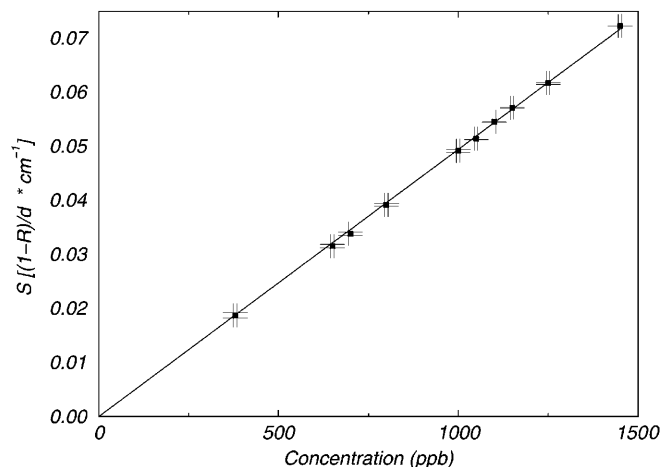


Fig. 4. Linearity plot of the CEA detector. For different ammonia concentrations the CEA spectrum is measured. The integrated absorption S , which is equal to the area under the CEA spectrum, is plotted versus the ammonia concentration measured with the chemiluminescence monitor. From these results a detection limit of the CEA technique for the selected ammonia transitions is determined to be 100 ppb (1 s), corresponding to a fractional absorption of $2 \times 10^{-8} \text{ cm}^{-1}$

tions of ammonia are needed. These measurements, however, are rather tedious, as they are time consuming due to the strong adhesive properties of ammonia (long stabilisation times). Therefore, we decided to extend the linearity curve by measuring absorptions of water. A spectral feature formed by two closely spaced water absorptions with line strengths of 9.10×10^{-5} and $3.04 \times 10^{-5} \text{ cm}^{-2} \text{ atm}^{-1}$ at respectively 6586.015 cm^{-1} and 6585.877 cm^{-1} [20] is measured at atmospheric pressure and the result is shown in Fig. 5. Even though there are no interfering ammonia absorptions in this frequency region, the whole system is flushed with dry air for 12 h in order to get rid of residual ammonia. The relative humidity and the temperature are measured inside the box with a relative humidity sensor and are 60% and 20°C , respectively. With this information the number density of water in the gas flow can be calculated. The spectrum is acquired in 8 s. The profile of the absorption contour is fitted, assuming identical Voigt profiles for the two transitions (dashed lines in Fig. 5). The linearity of the CEA sensor is tested for water and the plot is shown in the inset of Fig. 5. A clear linear dependence between the integrated CEA signal and the water concentration detected with the relative humidity sensor is observed. From these results the detection limit of the CEA technique for the examined water absorption is determined. A SNR equal to 1 is obtained when the water concentration in the gas flow is 100 ppm. This corresponds to a relative humidity of 1% at a temperature of 20°C .

In a CEA spectrum the absorption is expressed in units of $(1 - R)/d$ (see Figs. 3 and 5). Therefore, the integrated absorption in the linearity plots (Fig. 4 and the inset of Fig. 5) is also presented in units that depend on $(1 - R)/d$. For water, the integrated absorption cross-sections are precisely known [20]. As a result, we can determine $(1 - R)/d$ from the slope of the linearity plot for water. This provides us with the reflectivity of the mirrors; $R \approx 0.99971(3)$, which is in good agreement with the specified value. In return, this result shows that

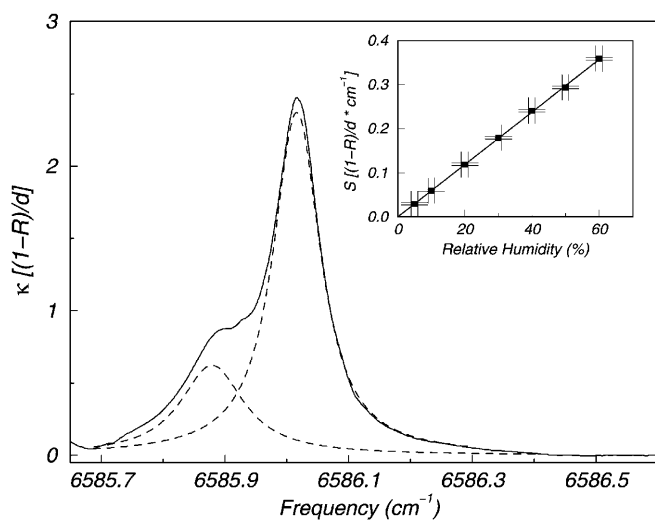


Fig. 5. CEA measurement of two closely spaced water lines that blend into one absorption feature at atmospheric pressure. The *dashed line* represents the two deconvoluted water absorptions. In the inset the results of the linearity measurement for the water absorptions are shown. A clear linear dependence is seen and a detection limit of 100 ppm (1 s) is found

CEA is an absolute absorption technique provided that the mirror reflectivity is known.

The sensitivity of the CEA technique for the detection of molecular species (here ammonia and water) can be enhanced in various ways. It can be seen from Figs. 3 and 5 that $\kappa(\nu)$ is plotted in units of $(1 - R)/d$. It is evident that by selecting a longer cavity length, a higher mirror reflectivity and/or absorptions with stronger line strengths, the detection limit can be lowered. Note that an increase of the cavity length will decrease the manageability of the set-up. For ammonia, there are several frequency regions with more intense absorption lines. In the $2.0\text{-}\mu\text{m}$ region, where compact diode lasers are presently available, cross sections five times stronger than in the $1.5\text{-}\mu\text{m}$ region have been reported [16]. Moreover, the fundamental rovibrational absorption bands of ammonia are even more intense and by probing transitions in these regions sub-ppb detection limits should be able to be obtained [21]. The resulting set-up, however, will be more complicated as there are no light sources for these rovibrational bands that are as easy to use as the commercially available diode lasers. If we choose the $0.7\text{--}2.0\text{ }\mu\text{m}$ region, we can calculate the sensitivity of the CEA technique for the detection of other molecules using the measured detection limits for ammonia and water, and the known absorption line strengths. For example, a detection limit for H_2S in the $1.5\text{-}\mu\text{m}$ region similar to the ammonia result is expected, as the absorption cross-sections are of the same order of magnitude [22]. The sensitivity of the CEA technique for HF detection in the $1.3\text{-}\mu\text{m}$ band is estimated to be in the low ppb range [21].

4 Summary

In this paper we demonstrate a highly sensitive and simple technique to monitor ammonia and water at atmospheric pressure using cavity-enhanced absorption spectroscopy. A compact diode laser operating at $1.5\text{-}\mu\text{m}$ is used as a light source. The ammonia and water measurements are calibrated independently using a chemiluminescence monitor and a relative humidity sensor, respectively. The ammonia detection limit of the CEA sensor is 100 ppb (1 s), at least one order of magnitude better than the previously reported sensitivities using open-path detection systems. For water a detection limit of 100 ppm (1 s) is shown. A clear linear dependence between the detected signal and the concentration is demonstrated. The absolute absorption measured in a CEA experiment depends on the value of the reflectivity of the cavity mirrors. From the CEA water measurements and the known water absorption cross-sections, the mirror reflectivity is calculated (which is in good agreement with the specified value). This indicates that the CEA technique can operate as a stand-alone sensor from which absolute gas concentrations can be obtained. In view of the scanning capabilities of the diode laser and the abundant absorptions of several molecules in the $1.5\text{-}\mu\text{m}$ region, it is in principle possible to construct a single-laser multigas sensor. The applicability of the CEA technique can readily be extended to other frequency regions, and thereby to the detection of a large variety of molecules.

Acknowledgements. Tobi Regts is acknowledged for the measurements in the climate chamber. This work is supported in part by the National Institute of Public Health and the Environment (RIVM).

References

1. G.P. Wyers, R.P. Otjes, J. Slanina: *Atmos. Environ.* **27A**, 2085 (1993)
2. R.A. Rooth, A.J.L. Verhage, L.W. Wouters: *Appl. Opt.* **29**, 3643 (1990)
3. H. Sauren, T. Regts, C. van Asselt, D. Bicanic: *Environ. Technol.* **12**, 719 (1991)
4. S.A. Trushin, B. Bunsegnes: *Phys. Chem. Phys.* **96**, 319 (1992)
5. M. Fehér, Y. Jiang, J.P. Maier, A. Miklós: *Appl. Opt.* **33**, 1655 (1994)
6. A. Miklós, M. Fehér: *Infrared Phys. Technol.* **37**, 21 (1996)
7. K.K. Lehman, S.L. Coy: *J. Chem. Soc., Faraday Trans.* **84**, 1389 (1988)
8. S.L. Coy, K.K. Lehman: *Spectrochim. Acta* **45A**, 47 (1989)
9. L. Lundsberg-Nielsen, F. Hegelund, F.M. Nicolaisen: *J. Mol. Spectrosc.* **162**, 230 (1993)
10. G. Berden, R. Peeters, G. Meijer: *Chem. Phys. Lett.* **307**, 131 (1999)
11. M. Ohtsu, H. Kotani, H. Tagawa: *Japan. J. Appl. Phys.* **22**, 1553 (1983)
12. M. Fehér, P.A. Martin, A. Rohrbacher, A.M. Soliva, J.P. Maier: *Appl. Opt.* **32**, 2028 (1993)
13. H. Ahlberg, S. Lundqvist, R. Tell, T. Andersson: *Spectrosc. Europe* **6**, 22 (1994)
14. G. Modugno, C. Corsi: *Infrared Phys. Technol.* **40**, 93 (1999)
15. P. Cancio, C. Corsi, F.S. Pavone, R.U. Martinelli, R.J. Menna: *Infrared Phys. Technol.* **36**, 987 (1995)
16. L. Sandström, S. Bäckström, H. Ahlberg, S. Höjer, A.G. Larsson: *Infrared Phys. Technol.* **39**, 69 (1998)
17. R.M. Mihalcea, M.E. Webber, D.S. Baer, R.K. Hanson, G.S. Feller, W.B. Chapman: *Appl. Phys. B* **67**, 283 (1998)
18. R. Engeln, G. Berden, R. Peeters, G. Meijer: *Rev. Sci. Instrum.* **69**, 3763 (1998)
19. H.J. Wiel: In *Messtechnik und Automatik* (VDI-Verlag GmbH, Düsseldorf 1974) pp. 52–60
20. R.A. Toth: *Appl. Opt.* **33**, 4851 (1994)
21. L.S. Rothman, R.R. Gamache, R.H. Tipping, C.P. Rinsland, M.A.H. Smith, D. Chris, V. Benner, M. Devi, J.-M. Flaud, C. Camy-Peyret, A. Perrin, A. Goldman, S.T. Massie, L.R. Brown, R.A. Toth: *J. Quant. Spectrosc. Radiat. Transfer* **48**, 469 (1992)
22. G. Modugno, C. Corsi, M. Gabrysch, M. Inguscio: *Opt. Commun.* **4755**, 76 (1998)